Can Ultrasound Biomicroscopy Be Used to Predict Accommodation Accurately?

Viswanathan Ramasubramanian, PhD; Adrian Glasser, PhD

ABSTRACT

PURPOSE: Clinical accommodation testing involves measuring either accommodative optical changes or accommodative biometric changes. Quantifying both optical and biometric changes during accommodation might be helpful in the design and evaluation of accommodation restoration concepts. This study aims to establish the accuracy of ultrasound biomicroscopy (UBM) in predicting the accommodative optical response (AOR) from biometric changes.

METHODS: Static AOR from 0 to 6 diopters (D) stimuli in 1-D steps were measured with infrared photorefraction and a Grand Seiko autorefractor (WR-5100 K; Shigiya Machinery Works Ltd., Hiroshima, Japan) in 26 human subjects aged 21 to 36 years. Objective measurements of accommodative biometric changes to the same stimulus demands were measured from UBM (VuMAX; Sonomed Escalon, Lake Success, NY) images in the same group of subjects. AOR was predicted from biometry using linear regressions, 95% confidence intervals, and 95% prediction intervals.

RESULTS: Bland–Altman analysis showed 0.52 D greater AOR with photorefraction than with the Grand Seiko autorefractor. Per-diopter changes in accommodative biometry were: anterior chamber depth (ACD): -0.055 mm/D, lens thickness (LT): +0.076 mm/D, anterior lens radii of curvature (ALRC): -0.854 mm/D, posterior lens radii of curvature (PLRC): -0.222 mm/D, and anterior segment length (ASL): +0.030 mm/D. The standard deviation of AOR predicted from linear regressions for various biometry parameters were: ACD: 0.24 D, LT: 0.30 D, ALRC: 0.24 D, PLRC: 0.43 D, ASL: 0.50 D.

CONCLUSIONS: UBM measured parameters can, on average, predict AOR with a standard deviation of 0.50 D or less using linear regression. UBM is a useful and accurate objective technique for measuring accommodation in young phakic eyes.

[*J Refract Surg.* 2015;31(4):266-273.]

Clinical accommodation testing involves objectively measuring accommodative optical changes or anterior segment accommodative biometric changes. Objective instruments to measure the accommodative optical response (AOR) include autorefractors,[1,2] refractometers,[3,4] infrared photorefraction,[5,6] or aberrometers.[7,8] Instruments that measure the AOR do not allow for visualization or quantification of the accommodative intraocular biometric changes that produce the AOR.

Accommodative biometric changes have been measured using A-scan ultrasound,[5] ultrasound biomicroscopy,[9,10] optical coherence tomography,[11] partial coherence interferometry,[12] Scheimpflug imaging,[13] and magnetic resonance imaging.[14] Biometric measurements of the ocular anterior segment during accommodation demonstrate and quantify the intraocular movements that lead to accommodation, but do not directly provide information on the AOR.

Prior studies[13,15,16] have related accommodative biometric changes to accommodative stimulus demands. When the accommodative biometry response is expressed as per-diopter of stimulus demand, this underestimates the true per-diopter of accommodative response changes due to the accommodative lag resulting from the depth of focus of the eye.[17] Hence, it is useful to measure both the AOR and the biometric changes to understand how the two are related. Currently, it is not possible to measure the accommodative optical and biometric changes with a single instrument. In a clinical setting, using two different instruments to measure the AOR and the biometric changes would be time-consuming and costly.

From the College of Optometry, University of Houston, Houston, Texas.

Submitted: July 30, 2014; Accepted: January 30, 2015

Supported by National Institutes of Health/National Eye Institute R01 EY017076 (AG) and National Institutes of Health/National Eye Institute P30 EY07551 (Core Grant to the University of Houston College of Optometry).

The authors have no financial or proprietary interest in the materials presented herein.

Correspondence: Adrian Glasser, PhD, College of Optometry, University of Houston, 4901 Calhoun Road, Houston, TX 77204. E-mail: aglasser@uh.edu

doi:10.3928/1081597X-20150319-06

Studies have measured accommodative biometric changes to demonstrate the mechanism of action and accommodative performance of an accommodative restoration strategy.[18] Although measuring and showing biometric movements of an accommodative intraocular lens (IOL), for example, can provide unequivocal objective evidence that the IOL accomplishes what is claimed of it, it can be difficult to relate the biometric measurements to how much accommodation this produces.

Several human,[5,12] monkey,[19,20] and in vitro[21,22] studies have shown linear correlations between AOR and accommodative biometric changes. These linear relationships allow the AOR to be estimated if the accommodative biometric changes are measured or known. If the AOR could be predicted from biometric measurements, then accommodation could be evaluated using only a single biometry instrument.

The current study was performed to determine how well ultrasound biomicroscopy (UBM) can be used to predict the AOR from anterior segment accommodative changes in a population of young phakic human subjects.

PATIENTS AND METHODS

In the volunteer subjects, AOR was first measured objectively with a Grand Seiko autorefractor (WR-5100 K; Shigiya Machinery Works Ltd., Hiroshima, Japan), then with infrared photorefraction. Then the accommodative biometric changes were measured to the same stimulus demands with UBM (VuMAX; Sonomed Escalon, Lake Success, NY) and A-scan ultrasound as described previously.[9] The study followed the tenets of the Declaration of Helsinki and was performed in accordance with a human subject protocol approved by the Commitee for Protection of Human Subjects at the University of Houston. Subjects were enrolled after passing a screening examination.[9] Subjects with refractive errors were corrected with spherical or toric soft contact lenses. The illumination in the examination room was dimmed to a similar level for all subjects for all procedures.

Grand Seiko Autorefractor

Baseline refraction and static AOR were measured objectively using the Grand Seiko autorefractor. The far target was a back-illuminated Snellen chart (Precision Vision, La Salle, IL) at 6 meters from the subject. The near target was a custom-designed back-illuminated letter chart suspended on a calibrated near-point rod attached to the Grand Seiko autorefractor. The far and near targets were aligned to ensure on-axis measurements in both conditions. Measurements were recorded in dim room illumination. Subjects viewed the far or near targets monocularly with the left eye through the Grand Seiko autorefractor open field beam splitter with their right eye occluded. Three refraction measurements were made for each stimulus demand from 0 to 8 diopters (D) in 1-D steps and the mean ± SD sphere at each stimulus demand was used for analysis. AOR was calculated as the difference in spherical refraction at each stimulus demand from the baseline.

To calculate the accuracy and noise of the Grand Seiko autorefractor, trial lenses from -5 to +2 D in 1-D steps were placed in front of the Grand Seiko model eye and 10 refraction measurements were taken with the Grand Seiko autorefractor with each trial lens. The induced and measured model eye refractions were strongly correlated (**Figure A1**, available in the online version of this article). Noise of the Grand Seiko autorefractor measurements calculated as the average standard deviations of all refraction measurements with all trial lenses was 0.009 D. Bland–Altman analysis showed a mean difference of +0.072 D (**Figure A2**).

Infrared Photorefraction

An aluminum frame was constructed (ITEM, Akron, OH) to perform photorefraction and ultrasound biomicroscopy measurements during accommodation on supine subjects.[9] The adjustable frame held a mirror for viewing a far target, a near target, a beam splitter, a photorefractor camera, and a hot mirror for the refraction measurements (**Figure 1A**). The subject lay supine, looking up, with the head stabilized with a gel head rest. Immediately in front of the viewing eye was a beam splitter oriented at 45°. The subject viewed the far target through this beam splitter or the near target reflected off to the side of the beam splitter. Only one of the far or near targets was illuminated at one time, so only one target was visible. Above the beam splitter was positioned a hot mirror that allowed the photorefraction camera to image the subject's eye as reflected in the infrared light off the hot mirror, while the subject could view the far target in visible light through the hot mirror. Above the hot mirror was a front silvered mirror oriented at 45°, which allowed the subject to view the far target that was projected on a screen on the wall (**Figure 1B**). A custom-designed illuminated near letter target was viewed reflected off a beam splitter. The near target could be moved on a meter stick to change the target vergence. A custom-developed photorefractor (inset in **Figure 1B**) was used to measure refraction of the left eye via a hot mirror.[23] All measurements with photorefraction were performed in dim room illumination.

A photorefraction trial lens calibration was performed on each subject at a working distance of 1

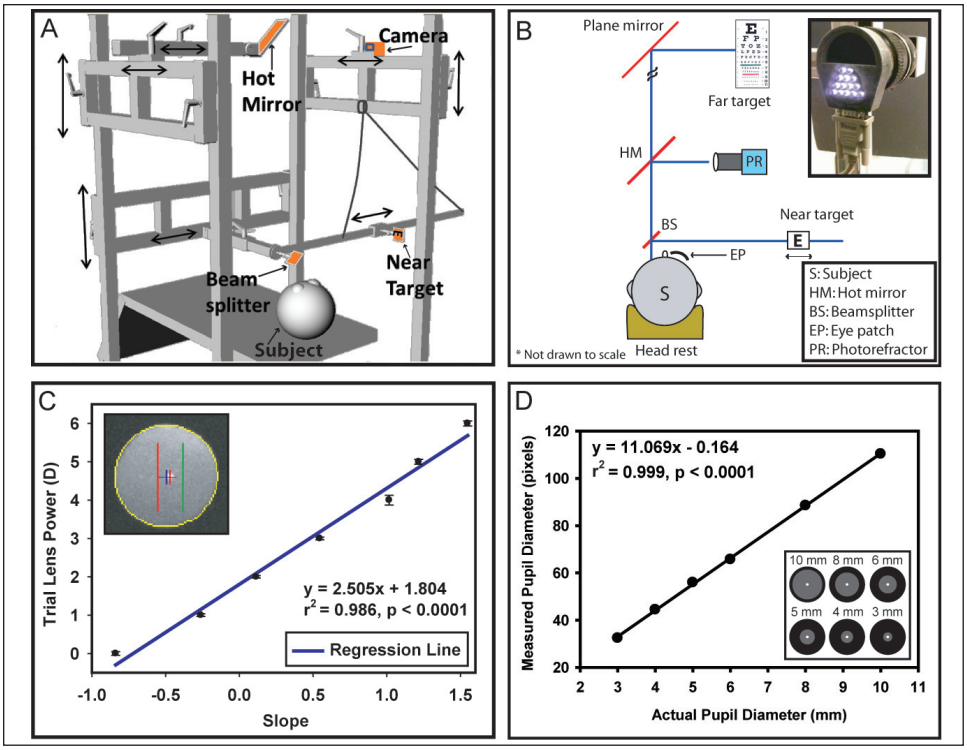

Figure 1. (A) An aluminum frame designed to hold various optical components for the study performed. (B) Experimental set-up for infrared photorefraction on the left eye. (C) An example of a trial lens calibration curve from a single subject. Inset is a Matlab analyzed (colored overlay) photorefraction image. The pixel intensity profiles are extracted along the red and green vertical lines. A circle fit to the pupil edge is shown in yellow. The blue and red crosses represent the positions of pupil center and the first Purkinje image. (D) Calibration function to calculate the pixel-to-mm conversion factor for photorefraction images. Inset shows the images of fixed pupil diameters used for this analysis.

meter. Photorefraction video sequences of the left eye were recorded at 30 Hz for 8 seconds for each trial lens (+8 to 0 D) in 1-D steps using custom-developed Matlab software (MathWorks, Natick, MA). During the trial lens calibration, subjects were asked to fixate on the far target using their right eye and to ignore the blur from the left eye produced by the trial lens.

For the photorefraction AOR measurements, the right eye was patched. The far and near targets were superimposed to ensure on-axis refraction of the left eye. Three 8-second photorefraction video sequences (each video containing 240 images) were recorded for each stimulus demand from 0 to +6 D in 1-D steps. All photorefraction videos were analyzed offline using custom-developed Matlab software. The software extracts pixel intensity values along the vertical pupil meridian (equal to 75% of the measured pupil diameter) (**Figure 1C** inset) and computes the slope of the linear regression fit to these intensity values.[24,25] The mean slope values for each trial lens were plotted against the trial lens power to obtain individual calibration curves (**Figure 1C**). The mean slope calculated from the videos during accommodation measurements was converted to refraction using the calibration function and accounting for the camera working distance. Accommodative optical response was calculated as the difference in spherical refraction at each stimulus demand from the baseline.

Pupil diameter was measured from the photorefraction images for all stimulus demands. Pixel-to-mm conversion factor for photorefraction images was calculated by imaging a series of printed pupils of known diameter (inset in **Figure 1D**). The slope of the linear regression equation was the pixel-to-mm conversion (1 mm = 11.069 pixels) factor. To compute the noise of the photorefraction system, trial lenses ranging from -1 to +5 D in 1-D steps were placed in front of a Heine ophthalmoscope trainer (Heine USA, Dover, NH) to get a calibration function (not shown) similar to the trial lens calibration described above. Mean ± SD of slope was calculated as the average SD of all slope values from all trial lens powers. From the calibration function, the range of refraction corresponding to 1 SD (a given x-value ± 0.5 × mean SD) of slope was calculated to represent noise of 0.022 D.

After the photorefraction measurements, UBM images of the left eye were captured while the subjects accommodated to a visual target with their right eye.[9] Accommodative changes in anterior chamber depth (ACD), lens thickness (LT), anterior and posterior lens radii of curvature (ALRC and PLRC), and anterior segment length (ASL) were measured from UBM images using custom-developed Matlab software.[9]

RESULTS

Twenty-six subjects (8 males and 18 females), aged 21 to 36 years (mean ± standard deviation [SD]: 24.15 ± 3.03 years), participated. Refractive errors ranged from -5.50 to +2.75 D (mean ± SD, -1.31 ± 2.03 D). Mean ±

SD of objectively measured accommodative amplitude using the Grand Seiko autorefractor was 5.86 ± 0.42 D (range: 4.93 to 7.10 D). Data from a single subject show a linear and reproducible stimulus-response function (**Figure B1**, available in the online version of this article). Photorefraction measured stimulus-response functions from this subject plateaued at higher stimulus demands and had larger standard deviations than those measured from the Grand Seiko autorefractor (**Figure B2**).

The population plots of the Grand Seiko autorefractor and photorefraction measured AOR showed a nonlinear relationship and saturation of photorefraction at higher stimulus demands (**Figures C1-C2**, available in the online version of this article). One subject had impossibly high photorefraction measured AOR due to smaller (and darker) and variable pupil diameters, so the data from that subject were excluded. Analysis of the data for all subjects showed linear stimulus-response functions with the Grand Seiko autorefractor but slopes greater than 1.0 for photorefraction in some subjects. As a consequence of the discrepancy between the Grand Seiko autorefractor and photorefraction, the Grand Seiko autorefractor measured AOR was used for all subsequent analyses. Pupil diameter decreased as a function of AOR measured with the Grand Seiko autorefractor (-0.487 mm/D) and photorefraction (-0.393 mm/D), respectively (**Figures C3-C4**).

UBM measured accommodative biometric changes as a function of Grand Seiko autorefractor measured AOR for each subject were fitted with linear regressions. Only data from subjects with statistically significant linear relationships were included in the population plots. The number of subjects with statistically significant linear relationships between AOR and UBM measured biometry were ACD (n = 25), LT (n = 26), ALRC (n = 26), PLRC (n = 25), and ASL (n = 14). All of the population plots for the five biometry parameters (ACD, LT, ALRC, PLRC, and ASL) had statistically significant linear correlations ($P < .0001$) (**Figure D**, available in the online version of this article). The mm/perdiopter slopes were ACD: -0.055 mm/D, LT: +0.076 mm/D, ALRC: -0.854 mm/D, PLRC: -0.222 mm/D, and ASL: +0.030 mm/D. There were no statistically significant correlations between the magnitude of refractive errors and the accommodative changes in UBM measured biometry parameters.

With accommodation, the anterior lens surface moves anteriorly linearly and the posterior lens surface moves posteriorly linearly ($P < .0001$) (**Figure D6**). The anterior and posterior lens surface movements contribute 63% and 37% of the change in lens thickness, respectively.

AOR was predicted from each of the UBM measured anterior segment biometry parameters for the population and for individual subjects using three methods: (1) directly from the linear regression lines, (2) using the 95% confidence intervals, and (3) using the 95% prediction intervals. The axes of each graph in **Figure D** were flipped so that biometry became the independent variable on the horizontal axis and AOR the dependent or predicted variable on the vertical axis such as shown for ACD in **Figure E1** (available in the online version of this article). Standard deviation of each of the UBM measured biometry parameters for the young subject population was calculated from 50 UBM images for each subject for each stimulus demand. None of the measured parameter SDs showed statistically significant relationships with stimulus demand in any individual subject; therefore, mean SD was calculated by taking the average SD of measured biometry parameters for all stimulus demands, for all trials, from all subjects. Mean SDs of UBM measured parameters were: ACD: 17.6 µm, LT: 29.4 µm, ALRC: 335 µm, PLRC: 158 µm, ASL: 34 µm as reported previously.[9]

From the linear regressions, the range of y-values (AOR) corresponding to 1 SD (a given x-value ± 0.5 × mean SD) of each UBM measured biometry parameter (eg, ACD) was calculated.

To predict the AOR from the 95% confidence interval, the equations of the upper and lower confidence intervals were computed. Because the 95% confidence interval lines separate toward the extremes, the range of AOR was calculated as the mean difference between the y-values from the upper and lower 95% confidence interval equations for all corresponding x-values. Matlab code was written to run a loop from the minimum to the maximum x-value in fixed steps (ACD, LT, ASL: 0.0001 mm; ALRC, PLRC: 0.001 mm) to calculate the range of AOR for each x-value. Larger step sizes were used for the ALRC and PLRC because the range of x-values was approximately 10 times larger than for the other biometry parameters. Mean, SD, maximum, minimum, and median of the range were calculated for each biometry parameter. A similar calculation of the range of AOR was performed using the equations for the 95% prediction intervals. The mean ranges of AOR from all three methods for the population data together with the standard deviations from the Grand Seiko autorefractor and photorefraction measurements of AOR are shown in **Table 1**. These standard deviations were calculated as the mean ± SD of AOR for all stimulus demands, for all trials, from all subjects.

For individual subjects with significant linear relationships between biometry changes and AOR, the mean ± SD of each UBM measured biometry parameter

TABLE 1
Standard Deviation of Predicted AOR From Young Population as a Whole[a]

Biometry	Linear Regression	95% Confidence Interval	95% Prediction Interval	PR: SD of AOR	GS: SD of AOR
ACD (n = 25)	0.24	0.37	3.05		
LT (n = 26)	0.30	0.34	2.89		
ALRC (n = 26)	0.24	0.46	3.66	0.20	0.14
PLRC (n = 25)	0.43	0.52	3.77		
ASL (n = 14)	0.50	0.82	4.55		

AOR = accommodative optical response; D = diopters; PR = photorefraction; SD = standard deviation; GS = Grand Seiko autorefractor; ACD = anterior chamber depth; LT = lens thickness; ALRC = anterior lens radius of curvature; PLRC = posterior lens radius of curvature; ASL = anterior segment length
[a]Although all parameters were measured in all participants' eyes, only data from participants who showed statistically significant linear relationships between the accommodative optical and biometric changes were used for the analyses.

TABLE 2
Standard Deviation of Predicted AOR From Individual Participants[a]

	Mean ± SD (D)		
Biometry	Linear Regression	95% Confidence Interval	95% Prediction Interval
ACD (n = 25)	0.29 ± 0.05	1.51 ± 0.75	3.20 ± 1.54
LT (n = 26)	0.36 ± 0.10	1.06 ± 0.46	2.25 ± 0.94
ALRC (n = 26)	0.37 ± 0.11	1.34 ± 0.58	2.85 ± 1.19
PLRC (n = 25)	0.79 ± 0.49	1.45 ± 0.74	3.12 ± 1.57
ASL (n = 14)	1.04 ± 0.43	2.15 ± 0.95	4.40 ± 1.77

AOR = accommodative optical response; D = diopters; PR = photorefraction; SD = standard deviation; ACD = anterior chamber depth; LT = lens thickness; ALRC = anterior lens radius of curvature; PLRC = posterior lens radius of curvature; ASL = anterior segment length
[a]Although all parameters were measured in all participants' eyes, only data from participants who showed statistically significant linear relationships between the accommodative optical and biometric changes were used for the analyses.

from all stimulus demands was calculated. Range of AOR was predicted from each subject's linear regression line for each measured biometry parameter (**Figure E2**). **Table 2** shows the mean ± SD of the predicted range of AOR from linear regressions from each measured biometry parameter from individual subjects. Root mean square error of AOR (predicted minus measured) was calculated from linear regressions for each subject for all UBM measured biometry parameters. Mean ± SD of root mean square error of predicted AOR from each UBM measured biometry parameter was: ACD: 0.41 ± 0.19 D, LT: 0.29 ± 0.12 D, ALRC: 0.36 ± 0.15 D, PLRC: 0.40 ± 0.20 D, and ASL: 0.55 ± 0.20 D. Mean ± SD of the mean range of predicted AOR from the 95% confidence and 95% prediction intervals from each subject for all UBM measured biometry parameters are shown in **Table 2**. The magnitude of AOR prediction errors was independent of the subject's refractive errors.

Linear regression equations used to calculate AOR independently from each of the UBM measured biometry parameters for the young subject population are shown in **Table 3**. AOR was calculated for each biometry parameter for each subject using the linear regression equations and the differences between the calculated and measured AOR is shown in **Table 3**.

DISCUSSION

Photorefraction overestimated the AOR compared to the Grand Seiko autorefractor measurements. This might be due to small pupils and therefore darker photorefraction reflexes in some subjects while accommodating to higher demands. A small pupil diameter allows only a limited number of pixels to be extracted from the pupil for the slope determination, which might account for a greater variance in the refraction measurement. The overestimation might also be due to the differences in the entrance pupil diameters used by these two instruments. The Grand Seiko autorefractor measurement is performed through a fixed 2.3-mm aperture regardless of the actual pupil diameter, whereas photorefraction as employed here always used 75% of the available pupil diameter.

Per-diopter of accommodative response changes in biometry from the current study are comparable to values reported in prior human and monkey accommodation studies (**Table 4**). The percentage contribution of

TABLE 3

AOR Predictions Using Linear Regression Equations From Biometry

Biometry	Population Linear Regression Equations to Predict AOR From Biometry	Absolute Difference Between Measured AOR and Predicted AOR (D)			
		Mean	SD	Minimum	Maximum
ACD	AOR = -13.405 × Δ ACD + 0.309	0.62	0.44	0.02	1.87
LT	AOR =+10.121 × Δ LT + 0.219	0.56	0.46	0.00	2.57
ALRC	AOR = -0.733 × Δ ALRC + 0.694	0.74	0.54	0.00	3.08
PLRC	AOR =-2.725 × Δ PLRC + 0.991	0.75	0.56	0.01	3.33
ASL	AOR =+14.678 × Δ ASL + 1.675	0.91	0.65	0.00	3.29

AOR = accommodative optical response; D = diopters; SD = standard deviation; Δ = accommodative change in; ACD = anterior chamber depth; LT = lens thickness; ALRC = anterior lens radius of curvature; PLRC = posterior lens radius of curvature; ASL = anterior segment length

TABLE 4

Comparison of Per-Diopter of Accommodative Response Changes in Anterior Segment Biometry From Prior Studies

Study	Subjects	Method Used to Measure Biometry	Per-Diopter Changes in Biometry (mm/D)				
			ACD	LT	ALRC	PLRC	ASL
Current study	Human	UBM	-0.055	+0.076	-0.853	-0.222	+0.030
Richdale et al.[14]	Human	OCT	N/A	+0.064	N/A	N/A	N/A
Sheppard et al.[29]	Human	3D MRI	N/A	+0.080	-0.630	-0.150	N/A
Hermans et al.[30]	Human	3D MRI	N/A	+0.061	-0.510	-0.140	N/A
Bolz et al.[12]	Human	PCI	-0.057	+0.072	N/A	N/A	+0.025
Ostrin et al.[5]	Human	A-scan	-0.051	+0.067	N/A	N/A	+0.017
Vilupuru and Glasser[20]	Monkey	CUB	-0.046	+0.063	N/A	N/A	+0.017

D = diopter; ACD = anterior chamber depth; LT = lens thickness; ALRC = anterior lens radius of curvature; PLRC = posterior lens radius of curvature; ASL = anterior segment length; UBM = ultrasound biomicroscopy; OCT = optical coherence tomography; N/A = not available; MRI = magnetic resonance imaging; PCI = partial coherence interferometry; CUB = continuous ultrasound biometry

posterior lens surface movement to the accommodative increase in lens thickness in the current study is higher than reported from prior human[5,12] and monkey studies.[20,26] A similar experiment was performed in prepresbyopic subjects aged 36 to 46 years and the results will be described in a separate manuscript.

The accommodative biometric changes measured in the current study are both qualitatively and quantitatively similar to results from prior studies. In particular, the anterior movement of the lens anterior surface and the posterior movement of the lens posterior surface contributing approximately 63% and 37%, respectively, of the total increase in lens thickness were comparable to prior studies.[5,12,20] Despite the fact that the current study was performed with subjects in a supine position, the nature of the accommodative response was similar to that shown previously in subjects in an upright posture. Thus, having subjects supine per se does not influence the accommodative response. Factors that may be more influential are the nature of the accommodative stimulus and how accommodation is stimulated and the overall comfort of the subjects. It may be more challenging to present compelling accommodative stimuli to subjects in a supine position and to have them comfortable with a scleral cup and fluid on the eye, but the system used in the current study was able to stimulate accommodation effectively. The fact that only 14 of the 26 subjects showed a significant linear change in ASL with accommodation is most likely due to the fact that the change in ASL with accommodation is small compared to the other biometric accommodative changes. The slope of the population linear regression line (**Figure D5**) for ASL is the smallest of the biometric changes. The data from the 12 subjects excluded from this analysis did not show significant linear changes in ASL with AOR. For a biometric parameter to offer some predictive ability, it must change systematically with accommodation.

The small accommodative changes that occur in ASL obviously make it the least suitable biometric parameter to use for making predictions of the AOR.

The primary goal of this study was to determine how accurately the AOR can be predicted in a population from UBM biometry measurements. Prior accommodation studies have reported linear correlations between refraction and biometry,[5,12,20] but have not attempted to predict the AOR from the measured biometry. In the current study, the linear regression method used the SD of the biometry measurements to predict the corresponding range of AOR. The range of the predicted AOR is smaller when the slope of the regression line is flatter and/or the mean ± SD of biometry is smaller. Using the 95% confidence interval to estimate the range of AOR takes account of the variance in the subject population. When the spread in the population data is smaller, the confidence interval is smaller and so the predicted range of AOR becomes smaller. The 95% prediction interval is wider than the confidence interval because it predicts 95% of the position of future data if the measurements were to be repeated. Accommodative optical response predictions from averaging the data from all individual subjects (**Table 2**) are slightly worse than predictions from the data from the population as a whole (**Table 1**) for all UBM measured biometry parameters. This might be due to the relatively stronger influence of a small number of data points on the slopes of the linear regressions in individual subjects and on the width of the 95% confidence and prediction intervals in individual subjects compared to the population plots.

Here, AOR was predicted independently from each UBM measured biometry parameter. An effort to predict the AOR using a multiple linear regression model fails because the strong linear correlations among all of the UBM measured accommodative biometry parameters[9] causes the multiple linear regression model to be unstable and therefore unsuitable to use.

Here, the AOR and biometric changes were not measured simultaneously. Hence, subjects could have accommodated to different degrees during sequential optical and biometric measurements. The consequence of this is that the linear relationship between AOR and biometry might not be as strongly correlated as they actually are. Also, UBM has limited axial resolution, which might have contributed to increased variance of biometry measurements. Factors affecting the variance of UBM measurements[9] in turn affect the AOR predictions. Simultaneous measurements of AOR and biometric changes using higher resolution imaging techniques such as anterior segment optical coherence tomography might offer better predictions.

Based on the current study, if accommodative changes in anterior segment biometry were measured, the linear regression equations provided (**Table 3**) could be used to calculate AOR in a young phakic subject population. On average, prediction errors from the linear regressions are less than 1 D for all biometry parameters, with LT being the best predictor. However, when predicting the AOR in this way, errors might occur due to the differences between the individual subjects' AOR and biometric response with that of the population. In the current study, although only data from subjects who had statistically significant linear relationship between optical and biometric changes were used for AOR prediction, almost all of the subjects had a statistically significant linear relationship for all UBM measured biometry parameters except ASL. Hence, it would be better to use ACD, LT, ALRC, or PLRC for AOR predictions and to not use ASL.

Predicting the AOR could be useful in instances where accommodative optical measurements may prove difficult or impossible due to the inability of an autorefractor or an aberrometer to measure a pseudophakic eye, for example, because of spurious light reflections from the IOL and/or miotic pupils.[27,28] Further investigation is required to test the validity of this prediction in prepresbyopic subjects with lower accommodative amplitudes. Application of this method may be important for evaluating accommodative ability in patients with accommodative IOLs where evaluating and understanding the accommodative movements of IOLs may be as important as measuring the AOR of the eye. However, the relationships between biometric movements and AOR in pseudophakic eyes would likely be different from the relationships shown here in young phakic eyes. Therefore, the relationships in eyes with specific types of IOLs would first have to be established for the predictions to be made.

AUTHOR CONTRIBUTIONS

Study concept and design (VR, AG); data collection (VR); analysis and interpretation of data (VR, AG); writing the manuscript (VR, AG); critical revision of the manuscript (VR); administrative, technical, or material support (AG); supervision (AG)

REFERENCES

1. Win-Hall DM, Houser J, Glasser A. Static and dynamic accommodation measured using the WAM-5500 autorefractor. *Optom Vis Sci.* 2010;87:873-882.
2. Wolffsohn JS, O'Donnell C, Charman WN, Gilmartin B. Simultaneous continuous recording of accommodation and pupil size using the modified Shin-Nippon SRW-5000 autorefractor. *Ophthalmic Physiol Opt.* 2004;24:142-147.
3. Win-Hall DM, Ostrin LA, Kasthurirangan S, Glasser A. Objective accommodation measurement with the Grand Seiko and Hartinger coincidence refractometer. *Optom Vis Sci.* 2007;84:879-887.

4. Wold JE, Hu A, Chen S, Glasser A. Subjective and objective measurement of human accommodative amplitude. *J Cataract Refract Surg.* 2003;29:1878-1888.
5. Ostrin L, Kasthurirangan S, Win-Hall D, Glasser A. Simultaneous measurements of refraction and A-scan biometry during accommodation in humans. *Optom Vis Sci.* 2006;83:657-665.
6. Kasthurirangan S, Glasser A. Influence of amplitude and starting point on accommodative dynamics in humans. *Invest Ophthalmol Vis Sci.* 2005;46:3463-3472.
7. Win-Hall DM, Glasser A. Objective accommodation measurements in prepresbyopic eyes using an autorefractor and an aberrometer. *J Cataract Refract Surg.* 2008;34:774-784.
8. Lopez-Gil N, Fernandez-Sanchez V, Legras R, Montes-Mico R, Lara F, Nguyen-Khoa JL. Accommodation-related changes in monochromatic aberrations of the human eye as a function of age. *Invest Ophthalmol Vis Sci.* 2008;49:1736-1743.
9. Ramasubramanian V, Glasser A. Objective measurement of accommodative biometric changes using ultrasound biomicroscopy. *J Cataract Refract Surg.* 2014;41:511-526.
10. Marchini G, Pedrotti E, Sartori P, Tosi R. Ultrasound biomicroscopic changes during accommodation in eyes with accommodating intraocular lenses: pilot study and hypothesis for the mechanism of accommodation. *J Cataract Refract Surg.* 2004;30:2476-2482.
11. Gambra E, Ortiz S, Perez-Merino P, Gora M, Wojtkowski M, Marcos S. Static and dynamic crystalline lens accommodation evaluated using quantitative 3-D OCT. *Biomed Opt Exp.* 2013;4:1595-1609.
12. Bolz M, Prinz A, Drexler W, Findl O. Linear relationship of refractive and biometric lenticular changes during accommodation in emmetropic and myopic eyes. *Br J Ophthalmol.* 2007;91:360-365.
13. Dubbelman M, van der Heijde GL, Weeber HA. Change in shape of the aging human crystalline lens with accommodation. *Vision Res.* 2005;45:117-132.
14. Richdale K, Sinnott LT, Bullimore MA, et al. Quantification of age-related and per diopter accommodative changes of the lens and ciliary muscle in the emmetropic human eye. *Invest Ophthalmol Vis Sci.* 2013;54:1095-1105.
15. Drexler W, Baumgartner A, Findl O, Hitzenberger CK, Fercher AF. Biometric investigation of changes in the anterior eye segment during accommodation. *Vision Res.* 1997;37:2789-2800.
16. van der Heijde GL, Beers APA, Dubbelman M. Microfluctuations of steady-state accommodation measured with ultrasonography. *Ophthalmic Physiol Opt.* 1996;16:216-221.
17. Nakatsuka C, Hasebe S, Nonaka F, Ohtsuki H. Accommodative lag under habitual seeing conditions: comparison between adult myopes and emmetropes. *Jpn J Ophthalmol.* 2005;49:189-194.
18. Marcos S, Ortiz S, Perez-Merino P, Birkenfeld J, Duran S, Jimenez-Alfaro I. Three-dimensional evaluation of accommodating intraocular lens shift and alignment in vivo. *Ophthalmology.* 2014;121:45-55.
19. Wendt M, Croft MA, McDonald J, Kaufman PL, Glasser A. Lens diameter and thickness as a function of age and pharmacologically stimulated accommodation in rhesus monkeys. *Exp Eye Res.* 2008;86:746-752.
20. Vilupuru AS, Glasser A. The relationship between refractive and biometric changes during Edinger-Westphal stimulated accommodation in rhesus monkeys. *Exp Eye Res.* 2005;80:349-360.
21. de Castro A, Birkenfeld J, Maceo B, et al. Influence of shape and gradient refractive index in the accommodative changes of spherical aberration in nonhuman primate crystalline lenses. *Invest Ophthalmol Vis Sci.* 2013;54:6197-6207.
22. Glasser A, Campbell MCW. Biometric, optical and physical changes in the isolated human crystalline lens with age in relation to presbyopia. *Vision Res.* 1999;39:1991-2015.
23. Tabernero J, Schaeffel F. More irregular eye shape in low myopia than in emmetropia. *Invest Ophthalmol Vis Sci.* 2009;50:4516-4522.
24. Schaeffel F, Wilhelm H, Zrenner E. Inter-individual variability in the dynamics of natural accommodation in humans: relation to age and refractive errors. *J Physiol.* 1993;461:301-320.
25. Roorda A, Campbell MC, Bobier WR. Slope-based eccentric photorefraction: theoretical analysis of different light source configurations and effects of ocular aberrations. *J Opt Soc Am A Opt Image Sci Vis.* 1997;14:2547-2556.
26. Vilupuru AS, Glasser A. Dynamic accommodative changes in Rhesus monkey eyes assessed with A-scan ultrasound biometry. *Optom Vis Sci.* 2003;80:383-394.
27. Glasser A. Restoration of accommodation: surgical options for correction of presbyopia. *Clin Exp Optom.* 2008;91:279-295.
28. Win-Hall DM, Glasser A. Objective accommodation measurements in pseudophakic subjects using an autorefractor and an aberrometer. *J Cataract Refract Surg.* 2009;35:282-290.
29. Sheppard AL, Evans CJ, Singh KD, Wolffsohn JS, Dunne MC, Davies LN. Three-dimensional magnetic resonance imaging of the phakic crystalline lens during accommodation. *Invest Ophthalmol Vis Sci.* 2011;52:3689-3697.
30. Hermans EA, Pouwels PJ, Dubbelman M, Kuijer JP, van der Heijde RG, Heethaar RM. Constant volume of the human lens and decrease in surface area of the capsular bag during accommodation: an MRI and Scheimpflug study. *Invest Ophthalmol Vis Sci.* 2009;50:281-289.

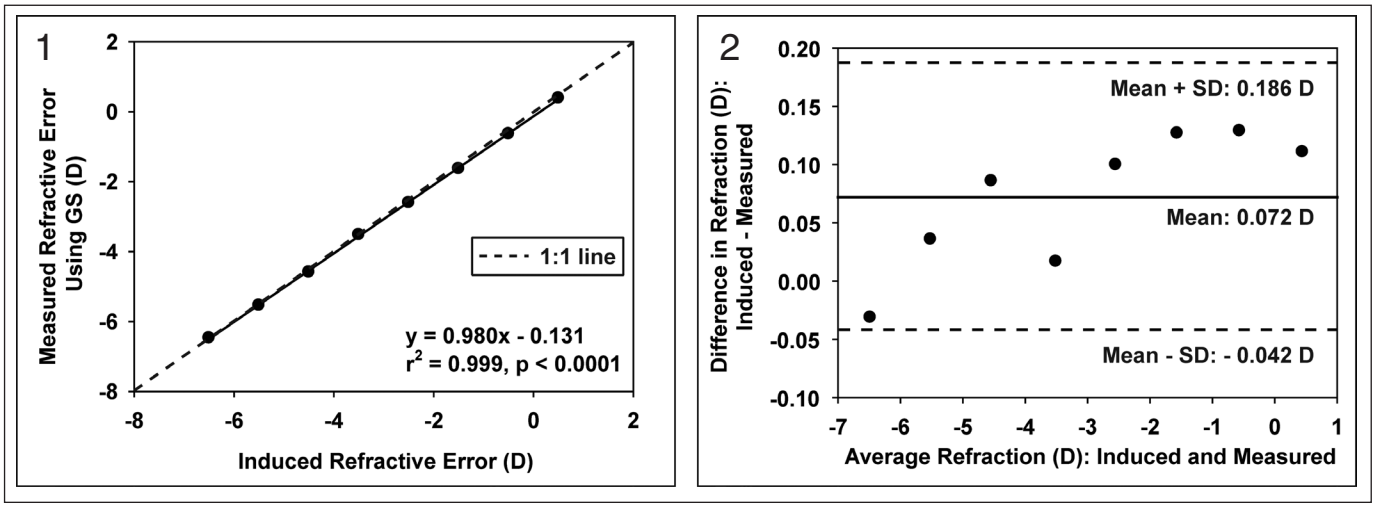

Figure A. (1) Comparison of the induced and measured model eye refraction using a Grand Seiko autorefractor (GS) (WR-5100 K; Shigiya Machinery Works Ltd., Hiroshima, Japan). Standard deviations (SDs) of GS measurements are small; hence the error bars plotted cannot be seen. (2) Bland–Altman plot shows a mean difference of 0.072 diopters (D) between induced and measured model eye refraction.

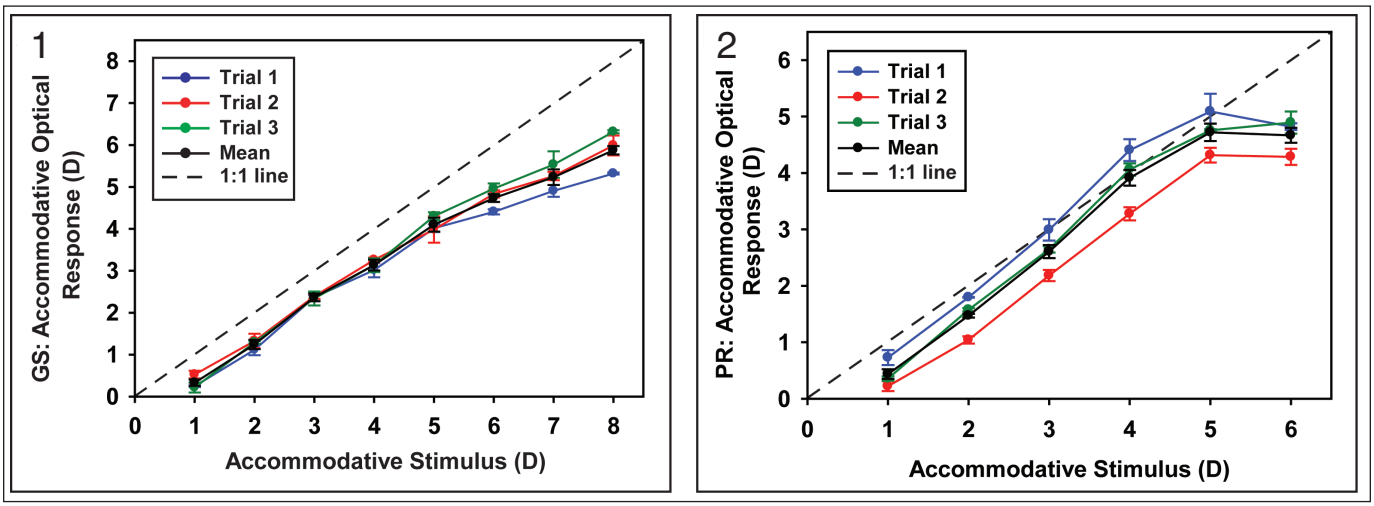

Figure B. (1) Grand Seiko autorefractor (GS) (WR-5100 K; Shigiya Machinery Works Ltd., Hiroshima, Japan) accommodative stimulus-response function from one subject from three separate trials. (2) Photorefraction (PR) accommodative stimulus-response function from the same subject for the three separate trials. Error bars represent ± 1 standard deviation from three measurements.

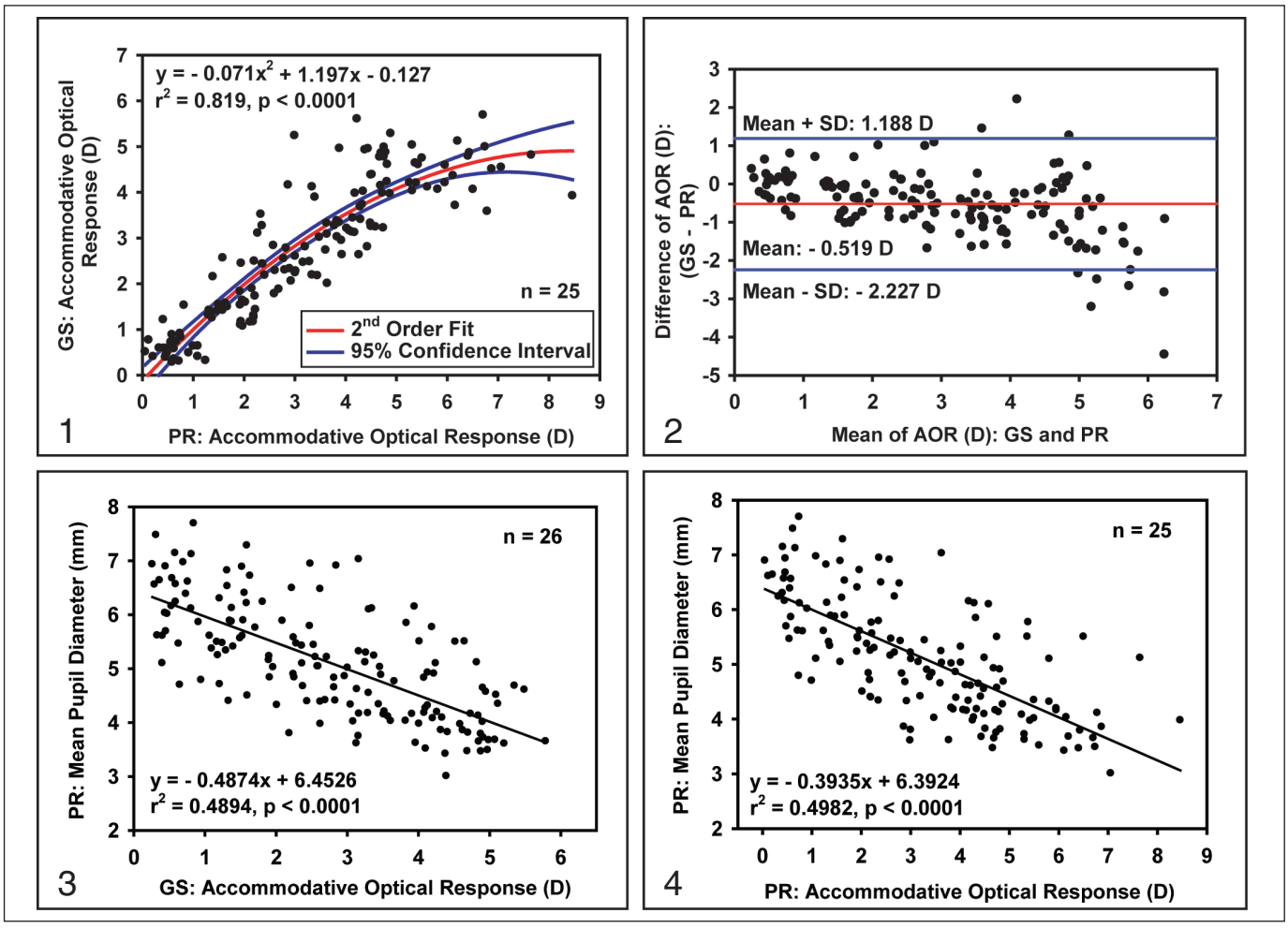

Figure C. (1) Comparison of accommodative optical responses (AOR) measured with Grand Seiko autorefractor (GS) (WR-5100 K; Shigiya Machinery Works Ltd., Hiroshima, Japan) and photorefraction (PR) from all subjects. (2) Bland-Altman comparison between GS and PR measured AOR with PR overestimating the GS measured AOR at higher stimulus demands. Comparison of PR measured pupil diameter as a function of (3) GS measured AOR and (4) PR measured AOR.

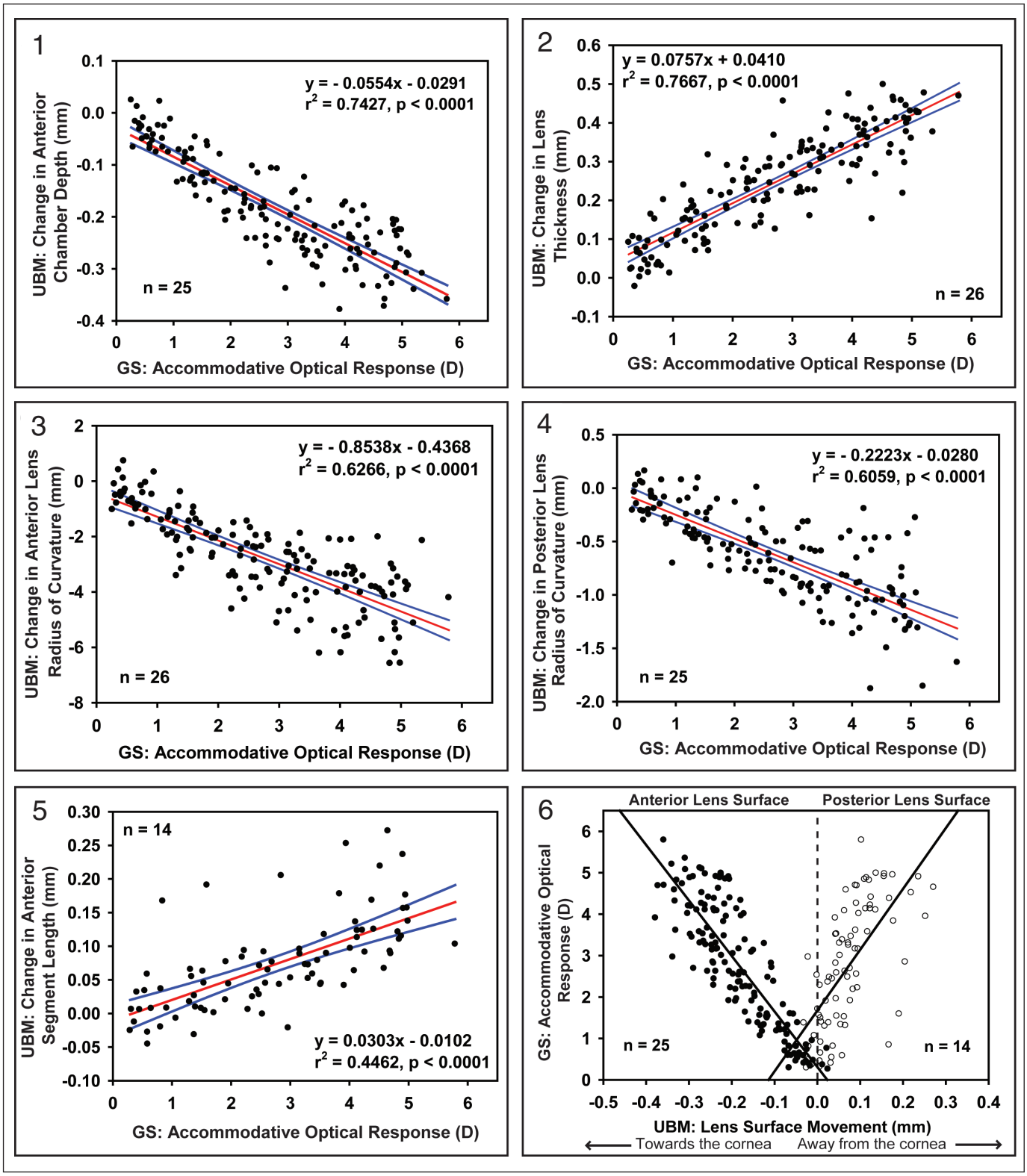

Figure D. Ultrasound biomicroscopy (UBM) measured ocular accommodative biometric changes as a function of Grand Seiko autorefractor (GS) (WR-5100 K; Shigiya Machinery Works Ltd., Hiroshima, Japan) measured accommodative optical response (AOR). With accommodation, (1) anterior chamber depth decreases, (2) lens thickness increases, (3) anterior lens radius of curvature decreases, (4) posterior lens radius of curvature decreases, and (5) posterior lens surface moves posteriorly. Each data point represents an average of all trials from each subject. 95% confidence intervals for the regression lines are shown. (6) Anterior (filled circles) and posterior (open circles) lens surface movement as a function of AOR ($P < .0001$).

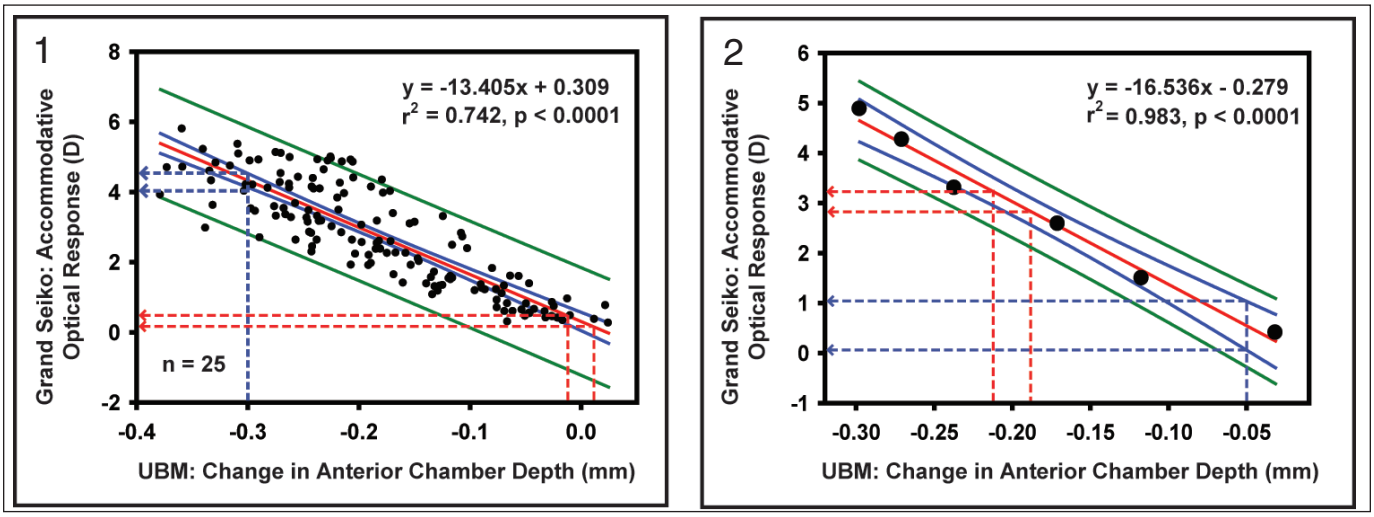

Figure E. The range of accommodative optical response (AOR) for (1) the study population as a whole and (2) a single individual subject. AOR was predicted from the linear regression (red solid line) and from the 95% confidence and prediction intervals (solid blue and green lines) from the biometry measurements. For each value on the horizontal axis, the range of AOR was calculated using the equations for the upper and lower 95% confidence (blue dashed line) and prediction intervals (not shown). Using the linear regression equation, the range of AOR was calculated using the standard deviation of the biometry measurements (red dashed line). UBM = ultrasound biomicroscopy